JCI The Journal of Clinical Investigation

# HDAC11 inhibition triggers bimodal thermogenic pathways to circumvent adipocyte catecholamine resistance

Emma L. Robinson, … , Jennifer L. Matsuda, Timothy A. McKinsey

*J Clin Invest.* 2023;133(19):e168192. https://doi.org/10.1172/JCI168192.

**Research Article** **Metabolism**

## Graphical abstract

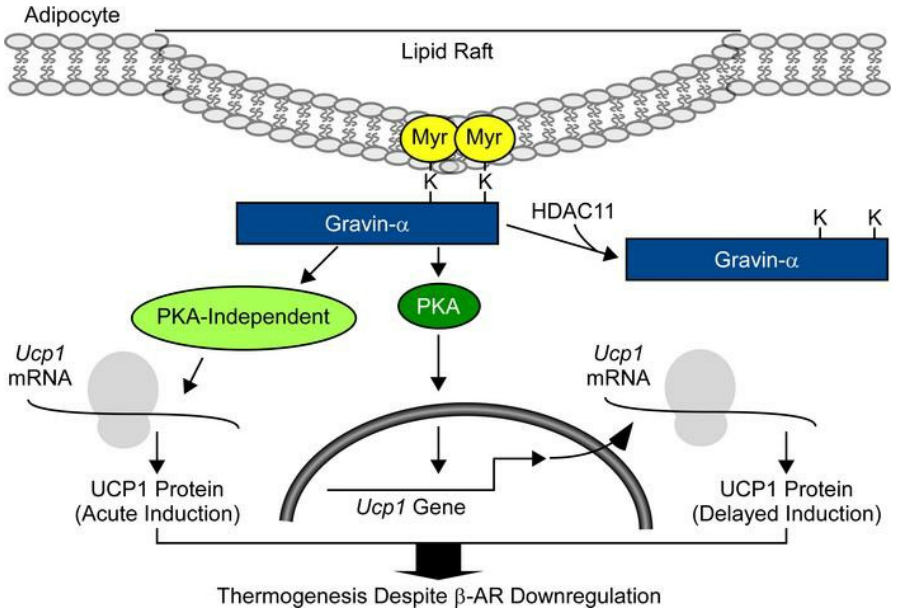

# HDAC11 inhibition triggers bimodal thermogenic pathways to circumvent adipocyte catecholamine resistance

**Emma L. Robinson,[1,2] Rushita A. Bagchi,[1,2] Jennifer L. Major,[1,2] Bryan C. Bergman,[3] Jennifer L. Matsuda,[4] and Timothy A. McKinsey[1,2]**

[1]Department of Medicine, Division of Cardiology, [2]Consortium for Fibrosis Research & Translation, and [3]Department of Medicine, Division of Endocrinology, Metabolism, and Diabetes, University of Colorado Anschutz Medical Campus, Aurora, Colorado, USA. [4]Department of Biomedical Research, National Jewish Health, Denver, Colorado, USA.

**Stimulation of adipocyte β-adrenergic receptors (β-ARs) induces expression of uncoupling protein 1 (UCP1), promoting nonshivering thermogenesis. Association of β-ARs with a lysine-myristoylated form of A kinase–anchoring protein 12 (AKAP12, also known as gravin-α) is required for downstream signaling that culminates in UCP1 induction. Conversely, demyristoylation of gravin-α by histone deacetylase 11 (HDAC11) suppresses this pathway. Whether inhibition of HDAC11 in adipocytes is sufficient to drive UCP1 expression independently of β-ARs is not known. Here, we demonstrate that adipocyte-specific deletion of HDAC11 in mice leads to robust induction of UCP1 in adipose tissue (AT), resulting in increased body temperature. These effects are mimicked by treating mice in vivo or human AT ex vivo with an HDAC11-selective inhibitor, FT895. FT895 triggers biphasic, gravin-α myristoylation–dependent induction of UCP1 protein expression, with a noncanonical acute response that is posttranscriptional and independent of protein kinase A (PKA), and a delayed response requiring PKA activity and new *Ucp1* mRNA synthesis. Remarkably, HDAC11 inhibition promotes UCP1 expression even in models of adipocyte catecholamine resistance where β-AR signaling is blocked. These findings define cell-autonomous, multimodal roles for HDAC11 as a suppressor of thermogenesis, and highlight the potential of inhibiting HDAC11 to therapeutically alter AT phenotype independently of β-AR stimulation.**

## Introduction

The prevalence of obesity in adults in the United States was recently estimated to be greater than 40%, and this number is expected to rise in coming years given that approximately 20% of children 2 to 19 years old are already obese or overweight (1, 2). Major advancements in pharmacotherapy for obesity have recently been realized, as exemplified by glucagon-like peptide-1 receptor agonists, which reduce appetite and function as incretin mimetics by promoting pancreatic insulin release (3). It may be possible to further increase the ability of antiobesity drugs to improve metabolic health through combination with agents that target distinct molecular mechanisms that impinge on adipose tissue (AT) to promote energy expenditure and ameliorate fat dysfunction, hallmarks of which are insulin resistance, inflammation, and fibrosis (4). In this regard, there is interest in developing drugs that directly augment brown AT (BAT) function and/or stimulate white AT (WAT) "beiging" as a means of treating metabolic disease (5).

**Conflict of interest:** TAM is a cofounder of Myracle Therapeutics, is on the scientific advisory boards of Artemes Bio and Eikonizo Therapeutics, received funding from Italfarmaco for an unrelated project, and has a subcontract from Eikonizo Therapeutics related to an SBIR grant from the NIH (HL154959).



**Submitted:** December 19, 2022; **Accepted:** August 3, 2023; **Published:** October 2, 2023.
**Reference information:** *J Clin Invest*. 2023;133(19):e168192.
https://doi.org/10.1172/JCI168192.

While the primary role of WAT is to store energy in the form of triglycerides in unilocular white adipocytes, brown adipocytes within BAT harbor small, multilocular lipid droplets and an abundance of mitochondria, which dissipate chemical energy as heat through nonshivering thermogenesis. Heat production by BAT is governed by uncoupling protein-1 (UCP1), which catalyzes mitochondrial proton leak and thereby uncouples electron transport from ATP synthesis (6–8). Beige adipocytes within WAT are similar to brown adipocytes in that they express UCP1, have multiple lipid droplets, and are rich in mitochondria (9). The existence of functional BAT in adult humans was confirmed by a series of positron-emission tomography studies, and body mass index and percentage body fat were found to negatively correlate with BAT abundance, suggesting the possibility that stimulating brown and beige adipocytes would be useful for the treatment of obesity and obesity-related disorders (10–13).

Pharmacological approaches to stimulate BAT and beiging of WAT in humans have focused on the use of $\beta_3$-adrenergic receptor ($\beta_3$-AR) agonists. $\beta_3$-AR stimulation directly enhances lipolysis and energy expenditure, and also triggers downstream signaling events that lead to potent induction of UCP1 expression in brown and white adipocytes (14). However, while $\beta_3$-AR agonists were shown to acutely increase energy expenditure and insulin sensitivity in humans, they have persistently failed to promote weight loss upon chronic administration (15–18). More recent human studies have employed mirabegron, a $\beta_3$-AR agonist that is

approved by the US Food and Drug Administration (FDA) for the treatment of overactive bladder. Acute administration of mirabegron was shown to stimulate BAT metabolic activity in humans, but typically required high doses of the agonist that resulted in cardiovascular side effects such as tachycardia and hypertension (19–22). In healthy young adults or older, obese and insulin-resistant humans, chronic mirabegron treatment improved glucose tolerance, but the drug only increased BAT activity in healthy individuals (23–25). The variable and limited effects of mirabegron on BAT activity in humans could be due to a greater reliance on $\beta_1$-AR and $\beta_2$-AR signaling in human versus murine AT, where $\beta_3$-AR predominates (20, 26). Alternatively, the restricted efficacy of mirabegron could be a consequence of catecholamine resistance, wherein chronic exposure to ligand and/or inflammatory cues results in a reduction in $\beta_3$-AR expression and signaling (27).

Histone deacetylase 11 (HDAC11) is a zinc-dependent enzyme that, paradoxically, functions as a robust lysine demyristoylase, with a catalytic efficiency greater than 10,000-fold higher for myristoyl-lysine versus acetyl-lysine (28–30). Whole-body deletion of HDAC11 in mice prevented weight gain and improved overall metabolic health in the face of chronic high-fat feeding, and the beneficial effects of HDAC11 knockout were linked to increased UCP1 expression in BAT and WAT (31, 32). Subsequent work revealed a cytoplasmic function for HDAC11 in the control of adipocyte $\beta_3$-AR signaling. By demyristoylating 2 lysine residues within the protein kinase A–binding (PKA-binding) domain of the scaffolding protein, A kinase–anchoring protein 12 (AKAP12, also known as gravin-α), HDAC11 prevents gravin-α:β-AR:PKA complexes from localizing to membrane lipid rafts that are required to stimulate downstream signaling that culminates in UCP1 expression (33). However, whether knockout and/or pharmacological inhibition of HDAC11 in adipocytes is sufficient to drive UCP1 expression independently of β-ARs remained known.

Here, we demonstrate that adipocyte-specific knockout of HDAC11 in mice profoundly induces expression of UCP1 in BAT and WAT, resulting in elevated body temperature. These effects are recapitulated by treating mice in vivo or human AT ex vivo with a pharmacological inhibitor of HDAC11. Adipocyte-specific HDAC11-knockout mice fed a high-fat diet (HFD) exhibit reduced weight gain and fat mass and improved glucose tolerance compared with controls. We provide evidence for biphasic, gravin-α myristoylation–dependent induction of UCP1 protein expression in adipocytes, with an early posttranscriptional response that is independent of PKA, and a later response requiring PKA and de novo *Ucp1* mRNA synthesis. HDAC11 inhibition stimulates UCP1 expression even in the setting of catecholamine resistance where β-AR signaling is blocked. These findings define cell-autonomous, multimodal roles for HDAC11 in the repression of UCP1 expression. Furthermore, the data underscore the potential of inhibiting HDAC11 to bypass catecholamine resistance and directly modulate AT phenotype in the context of obesity.

## Results

*Adipocyte-specific knockout of HDAC11 in mice is sufficient to induce UCP1 protein expression and promote thermogenesis*. Global deletion of HDAC11 in mice enhances UCP1 expression in AT (31, 32). To determine whether HDAC11 is a cell-autonomous repressor of thermogenic gene expression, mice harboring a conditional allele with *loxP* sites flanking exon 2 of the *Hdac11* gene were generated (Figure 1A). These *Hdac11*$^{fl/fl}$ mice were crossed with mice containing a transgene of the adiponectin promoter driving constitutive expression of Cre recombinase (*Adipoq-Cre*) to yield adipocyte-specific *Hdac11*–conditional knockout (*Hd11*$^{cKO}$) mice; *Hdac11*$^{fl/fl}$ mice served as controls (Figure 1, B–D). HDAC11 protein levels were greatly reduced in epididymal WAT (eWAT), inguinal WAT (ingWAT), and BAT of *Hd11*$^{cKO}$ mice compared with controls (Figure 1, E and F). Genetic deletion of HDAC11 in adipocytes led to marked induction of UCP1 protein expression in each of these AT depots (Figure 1, E–G).

To further address the cell-autonomous function of HDAC11, preadipocytes were isolated from the stromal vascular fraction of ingWAT from WT and *Hdac11*$^{fl/fl}$ mice and cultured in the absence or presence of recombinant cell-permeable Cre recombinase (Figure 1H). Remarkably, incubation of *Hd11*$^{fl/fl}$ preadipocytes with Cre for only 5 hours led to a dramatic reduction in HDAC11 protein abundance, which correlated with strong induction of UCP1 protein expression (Figure 1I).

As UCP1 functions to facilitate nonshivering thermogenesis, differences in core body temperature were examined in *Hd11*$^{cKO}$ and *Hd11*$^{fl/fl}$ control mice exposed to 4°C for 24 hours following 5 days of acclimatization at thermoneutrality (28°C–30°C) (Figure 1J). Compared with controls, *Hd11*$^{cKO}$ mice had higher core body temperature at baseline and throughout the 24-hour cold challenge (Figure 1K). Analysis of AT following necropsy revealed decreased WAT and increased BAT abundance and evidence of WAT beiging in *Hd11*$^{cKO}$ mice compared with controls (Figure 1, L and M). Together, these findings establish that HDAC11 serves an adipocyte-autonomous role in the control of AT thermogenic protein expression and remodeling.

*Adipocyte-specific knockout of HDAC11 in mice attenuates HFD-induced weight gain and glucose intolerance*. To assess the impact of adipocyte-specific HDAC11 deletion on changes in body composition in response to caloric excess, *Hd11*$^{cKO}$ mice and *Hd11*$^{fl/fl}$ controls were fed normal chow or an HFD for 16 weeks. Weight gain was reduced approximately 26% in *Hd11*$^{cKO}$ mice compared with controls, and this correlated with an approximately 24% decrease in fat mass, as determined by quantitative magnetic resonance imaging (Supplemental Figure 1, A and B; supplemental material available online with this article; https://doi.org/10.1172/JCI168192DS1); no differences in lean mass were observed between HFD-fed *Hd11*$^{cKO}$ and control mice (Supplemental Figure 1C). Glucose tolerance was also enhanced in *Hd11*$^{cKO}$ mice compared with controls (Supplemental Figure 1D). These data indicate that adipocyte-specific deletion of HDAC11 confers general metabolic benefit in the setting of HFD feeding, although expanded testing will be needed to corroborate these findings.

*Selective pharmacological inhibition of HDAC11 in mice is sufficient to induce thermogenesis and UCP1 expression*. To address the therapeutic potential of inhibiting HDAC11 to alter AT phenotype, mice were treated with a highly selective HDAC11 inhibitor (FT895) or vehicle control, for 5 days at thermoneutrality prior to a 24-hour 4°C challenge (Figure 2A). Mice pretreated with FT895 had a higher

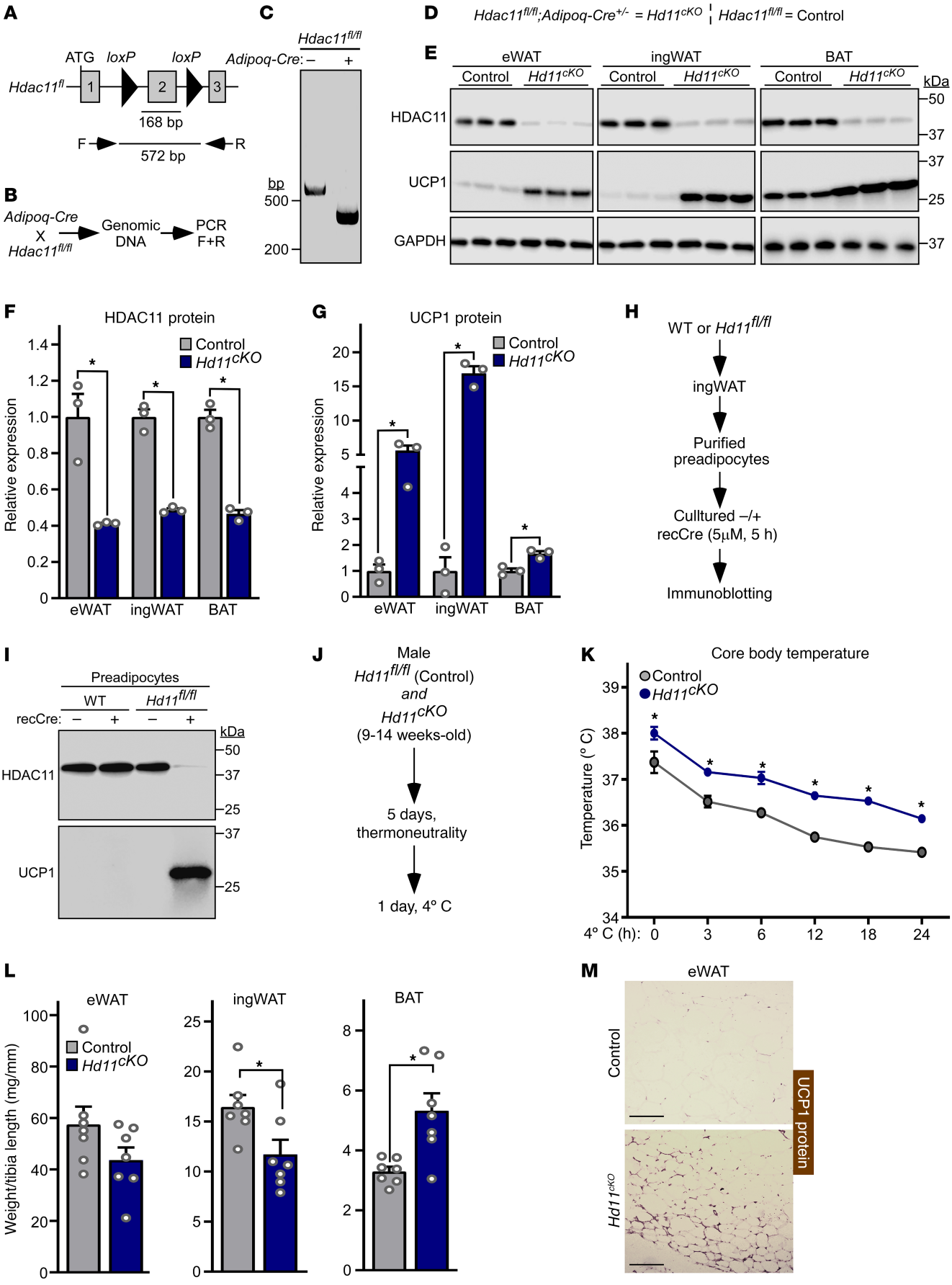
A
ATG loxP loxP
Hdac11fl
1 2 3
168 bp
F R
572 bp
B
Adipoq-Cre
X
Hdac11fl/fl
Genomic DNA
PCR F+R
C
Hdac11fl/fl
Adipoq-Cre: – +
bp
500
200
D
Hdac11fl/fl;Adipoq-Cre+/- = Hd11cKO
Hdac11fl/fl = Control
E
eWAT ingWAT BAT
Control Hd11cKO Control Hd11cKO Control Hd11cKO
kDa
HDAC11
UCP1
GAPDH
50
37
37
25
37
F
HDAC11 protein
Control
Hd11cKO
Relative expression
eWAT ingWAT BAT
G
UCP1 protein
Control
Hd11cKO
Relative expression
eWAT ingWAT BAT
H
WT or Hd11fl/fl
ingWAT
Purified preadipocytes
Culltured –/+ recCre (5μM, 5 h)
Immunoblotting
I
Preadipocytes
WT Hd11fl/fl
recCre: – + – +
kDa
HDAC11
UCP1
50
37
25
37
25
J
Male
Hd11fl/fl (Control)
and
Hd11cKO
(9-14 weeks-old)
5 days, thermoneutrality
1 day, 4° C
K
Core body temperature
Control
Hd11cKO
Temperature (° C)
4° C (h): 0 3 6 12 18 24
L
eWAT ingWAT BAT
Control
Hd11cKO
Weight/tibia length (mg/mm)
M
eWAT
Control
Hd11cKO
UCP1 protein

**Figure 1. Adipocyte-specific knockout of HDAC11 in mice is sufficient to induce UCP1 protein expression and promote thermogenesis.** (**A**) Schematic representation of the *Hdac11*-floxed allele (*Hdac11$^{fl}$*), with *loxP* sites flanking the 162 base pair (bp) exon 2; the predicted size of the resulting PCR product generated from genomic DNA and forward (F) and reverse (R) primers is shown. (**B**) Schematic representation of the cross between adiponectin promoter–driven Cre recombinase (*Adipoq-Cre*) transgenic mice and *Hdac11$^{fl/fl}$* mice and the genomic DNA PCR approach to assessing excision of *Hdac11* exon 2. (**C**) Genomic DNA PCR products from *Hdac11$^{fl/fl}$* mice without (–) and with (+) the *Adipoq-Cre* transgene. (**D**) Diagram describing the genotype and definition of the adipocyte-specific conditional *Hdac11*-KO (*Hd11$^{cKO}$*) and control *Hd11$^{fl/fl}$* mice. (**E**) Immunoblot analysis of HDAC11 and UCP1 protein in epididymal white adipose tissue (eWAT), inguinal white adipose tissue (ingWAT), and interscapular brown adipose tissue (BAT) from 10- to 12-week-old control and *Hdac11$^{cKO}$* mice. GAPDH served as a loading control; $n = 3$ biological replicates/group. (**F** and **G**) Densitometric analysis of HDAC11 and UCP1 protein in **E**, normalized to GAPDH and plotted relative to controls. Data are depicted as mean + SEM, with $^*P < 0.05$ as determined by 2-tailed, unpaired *t* test. (**H**) Schematic representation of the cell culture experiment with recombinant Cre recombinase (recCre). (**I**) Immunoblot analysis of HDAC11 and UCP1 protein in preadipocytes. (**J**) Schematic representation of the 24-hour 4°C challenge experiment. (**K**) Core body temperature over time. Data are depicted as mean ± SEM, with $^*P < 0.05$ vs. control mice at a given time as determined by 2-way ANOVA with Šidák's multiple-comparison test; $n = 7$ biological replicates/group. (**L**) Adipose tissue weight, normalized to tibia length, determined after the 24-hour 4°C challenge. Data are depicted as mean + SEM, with $^*P < 0.05$ as determined by 2-tailed, unpaired *t* test. (**M**) Immunohistochemistry of UCP1 protein in eWAT from mice sacrificed following the 24-hour 4°C challenge. Scale bars: 200 μm.

core body temperature at baseline and throughout the 4°C challenge (Figure 2B). Furthermore, compared with controls, mice treated with FT895 had reduced WAT and increased BAT abundance, and had profoundly augmented expression of UCP1 protein in eWAT, ingWAT, and BAT (Figure 2, C–E). These findings illustrate that pharmacological inhibition of HDAC11 catalytic activity phenocopies genetic deletion of HDAC11 in adipocytes, resulting in enhanced thermogenesis in association with strong induction of UCP1 protein expression and reduced remodeling of both WAT and BAT.

*HDAC11 triggers biphasic induction of UCP1 protein expression through posttranscriptional and transcriptional mechanisms.* Cultured adipocytes were used to elucidate the mechanism(s) by which HDAC11 inhibition induces UCP1 protein expression. Consistent with findings made with AT in vivo, treatment of differentiated murine white-like adipocytes, 3T3-L1 cells, with FT895 for 1 hour led to robust induction of UCP1 protein expression (Figure 3, A–C). Evaluation of primary adipocytes from WT and whole-body *Hdac11*-knockout mice established that FT895 stimulates UCP1 expression by inhibiting HDAC11 as opposed to through an off-target action since, compared with WT cells, UCP1 abundance was elevated at baseline in *Hdac11*-knockout adipocytes and not further increased by the inhibitor (Supplemental Figure 2). FT895 also stimulated UCP1 protein expression in HIB1B adipocytes, which exhibited higher basal UCP1 expression due to their brown adipocyte–like phenotype, and promoted expression of UCP1 in cultured primary human subcutaneous adipocytes (Figure 3, D–F).

Time course experiments were performed to define the kinetics of UCP1 induction following HDAC11 inhibition. UCP1 protein expression was dramatically upregulated as early as 5 minutes following FT895 treatment and was sustained 20 hours after exposure to the HDAC11 inhibitor in both 3T3-L1 and HIB1B adipocytes (Figure 3G). Rapid induction of UCP1 protein expression was also observed in primary human subcutaneous adipocytes exposed to FT895 (Figure 3H). Parallel gene expression analyses with 3T3-L1 and human adipocyte homogenates revealed that FT895 stimulated *Ucp1* mRNA expression beginning 60 minutes following treatment, suggesting that UCP1 protein induction following 5 minutes of FT895 exposure occurs through a posttranscriptional mechanism (Figure 3, I and J). To address this possibility, studies were performed with actinomycin D, which blocks gene transcription, and cycloheximide, which suppresses protein translation. Pretreatment with actinomycin D had no effect on UCP1 protein induction following 5 minutes of FT895 treatment, but substantially reduced UCP1 protein abundance following 60 minutes of HDAC11 inhibition (Figure 4, A and B). In contrast, cycloheximide pretreatment strongly reduced UCP1 induction at both time points (Figure 4, A and B). These data suggest that HDAC11 inhibition stimulates adipocyte UCP1 protein expression in a biphasic and bimodal manner, with acute induction occurring through a posttranscriptional mechanism, and delayed induction requiring de novo *Ucp1* mRNA synthesis.

*Biphasic UCP1 induction upon HDAC11 inhibition is dependent on gravin-α lysine myristoylation.* Myristoylation of the anchoring protein, gravin-α, on lysine residues 1502 and 1505 drives gravin-α:$\beta_3$-AR complexes into caveolin-rich lipid rafts to promote downstream PKA signaling (33). Conversely, demyristoylation of gravin-α by HDAC11 blocks $\beta_3$-AR signaling (Figure 5A). A click chemistry method with biotinylated myristic acid alkyne (Alk-12) confirmed that gravin-α was myristoylated in 3T3-L1 adipocytes following treatment with FT895 for 5 and 60 minutes (Figure 5, B and C).

To address the role of gravin-α and its myristoylation in the control of acute and chronic UCP1 protein induction following HDAC11 inhibition, endogenous gravin-α expression was knocked down in mouse 3T3-L1 adipocytes using short hairpin RNA (shRNA), and WT or a myristoylation-resistant version of rat gravin-α (K1502/1505R [KK/RR]) was subsequently ectopically expressed in the cells (Figure 6A). Knockdown of endogenous gravin-α dramatically reduced UCP1 protein induction following 5 and 60 minutes of FT895 treatment, and adding back WT, but not KK/RR, rescued UCP1 expression (Figure 6B). These findings correlated with stimulation of PKA signaling in the cells, with 5 and 60 minutes of FT895 treatment promoting PKA substrate phosphorylation in a manner that was dependent on site-specific myristoylation of gravin-α (Figure 6C).

A co-immunoprecipitation (co-IP) study was performed to determine whether HDAC11 inhibition alters association of PKA subunits with gravin-α. Association of PKA catalytic subunits (α and β), and the RII-α regulatory subunit, with FLAG-tagged gravin-α was readily detected in 3T3-L1 adipocytes, and these interactions were unchanged upon HDAC11 inhibition with FT895 (Supplemental Figure 3, A and B). Thus, HDAC11 inhibition does not appear to activate adipocyte PKA signaling by altering association of subunits of this kinase complex with the gravin-α scaffold.

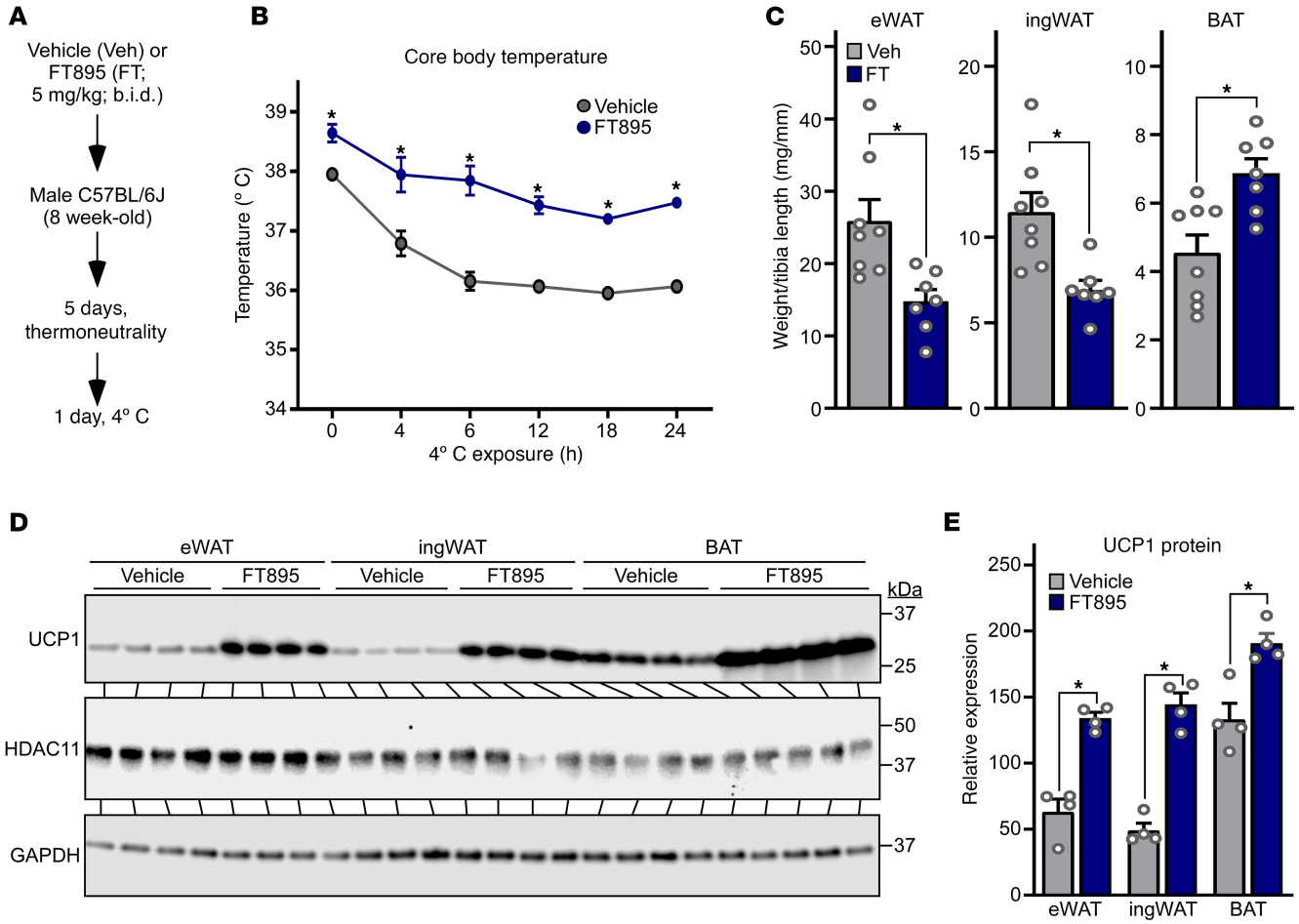


**Figure 2. Selective pharmacological inhibition of HDAC11 in mice is sufficient to induce thermogenesis and UCP1 expression.** (**A**) Schematic representation of the 24-hour 4°C challenge experiment employing the selective HDAC11 inhibitor, FT895. (**B**) Core body temperature was determined at the indicated times. Data are depicted as mean ± SEM, with $*P < 0.05$ vs. vehicle-treated mice at a given time as determined by 2-way ANOVA with Šidák's multiple-comparison test; vehicle ($n = 8$ biological replicates) and FT895 ($n = 7$ biological replicates). (**C**) Epididymal white adipose tissue (eWAT), inguinal white adipose tissue (ingWAT), and interscapular brown adipose tissue (BAT) weights, normalized to tibia length, determined upon necropsy after the 24-hour 4°C challenge. Data are depicted as mean + SEM, with $*P < 0.05$ as determined by 2-tailed, unpaired *t* test. (**D**) HDAC11 and UCP1 protein levels were assessed by immunoblotting with homogenates of AT obtained from mice sacrificed after the 24-hour 4°C challenge; $n = 4$ biological replicates/group. (**E**) Densitometric analysis of HDAC11 and UCP1 protein in **D**, normalized to GAPDH. Data are depicted as mean + SEM, with $*P < 0.05$ as determined by 2-tailed, unpaired *t* test.

*Inhibition of HDAC11 stimulates PKA-independent and PKA-dependent induction of UCP1 expression.* To determine whether acute and delayed UCP1 protein induction following HDAC11 inhibition are dependent on PKA signaling, which is the canonical pathway for stimulation of thermogenic gene expression, 3T3-L1 cells were treated with FT895 in the absence or the presence of the PKA inhibitor, H89 (Figure 7A). H89 administration had a limited effect on UCP1 protein induction following 5 minutes of FT895 treatment, but dramatically suppressed UCP1 expression in cells treated with the HDAC11 inhibitor for 60 minutes (Figure 7, B and C). Immunoblotting with an anti–phospho-PKA-substrate antibody confirmed the ability of H89 to effectively block FT895-mediated induction of general PKA signaling at both time points (Figure 7D). A time course experiment revealed PKA-independent induction of UCP1 for up to 30 minutes following treatment of 3T3-L1 adipocytes with FT895 (Supplemental Figure 4, A–C). Furthermore, PKA-independent and -dependent upregulation of UCP1 protein was observed in undifferentiated 3T3-L1 preadipocytes after 5 and 60 minutes of exposure to FT895, respectively (Supplemental Figure 5, A and B).

Analysis of RNA from independent samples demonstrated that H89 blocked FT895-mediated induction of *Ucp1* mRNA expression in mature 3T3-L1 adipocytes following 60 minutes of treatment; consistent with prior results, no induction of *Ucp1* mRNA expression was noted after 5 minutes of treatment with the HDAC11 inhibitor (Figure 7E). Thus, although induction of UCP1 protein expression following treatment with FT895 for 5 and 60 minutes is dependent on gravin-α myristoylation, and PKA is activated by the HDAC11 inhibitor at each time point, only the 60-minute response requires the activity of the kinase. This requirement is likely due to PKA-mediated stimulation of *Ucp1* mRNA synthesis.

*HDAC11 inhibition triggers UCP1 induction and PKA signaling in murine models of adipocyte catecholamine resistance.* Although the $\beta_3$-AR is not regulated by classical phosphorylation-dependent

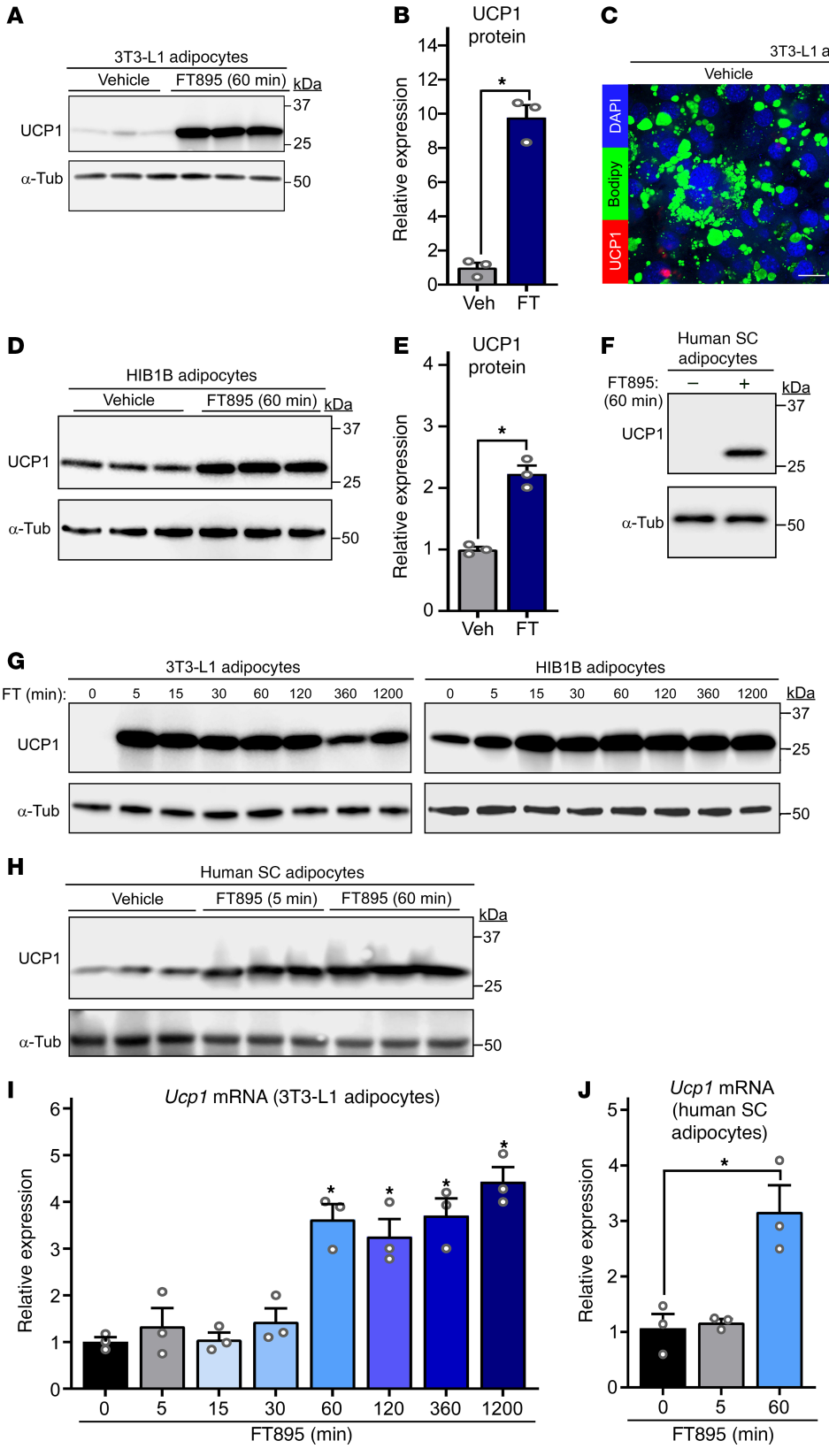


**Figure 3. HDAC11 inhibition triggers induction of UCP1 protein and mRNA expression in cultured adipocytes.** (**A**) Immunoblot analysis of UCP1 protein in 3T3-L1 white adipocytes treated with vehicle control or FT895 for 60 minutes; α-tubulin (α-Tub) served as a loading control; *n* = 3 technical replicates/condition. (**B**) Densitometric analysis of UCP1 expression in **A**, normalized to α-tubulin and plotted as fold-change relative to untreated controls. Data are presented as mean + SEM, with **P* < 0.05 by 2-tailed, unpaired *t* test. (**C**) Indirect immunofluorescence analysis of UCP1 protein (red) in 3T3-L1 adipocytes treated with vehicle control or FT895 for 60 minutes. Nuclei and lipid droplets were costained using DAPI (blue) and BODIPY (green), respectively. Scale bars: 10 μm. (**D**) Immunoblot analysis with homogenates of HIB1B brown adipocytes treated with vehicle control or FT895 for 60 minutes; *n* = 3 technical replicates/condition. (**E**) Densitometric analysis of UCP1 expression in **D**, normalized to α-tubulin and plotted as fold-change relative to untreated controls. Data are presented as mean + SEM, with **P* ≤ 0.05 by 2-tailed, unpaired *t* test. (**F**) Immunoblot analysis with homogenates of cultured human subcutaneous (SC) adipocytes treated with FT895 for 60 minutes. (**G**) Immunoblot analysis with homogenates of 3T3-L1 adipocytes (left) and HIB1B adipocytes (right) treated with FT895 for the indicated times. (**H**) Immunoblot analysis with homogenates of cultured human SC adipocytes treated with FT895 for 5 and 60 minutes; *n* = 3 technical replicates/condition. *Ucp1* mRNA expression in 3T3-L1 adipocytes (**I**) or human SC adipocytes (**J**) treated with FT895 for the indicated times was determined by qRT-PCR. Data were normalized to *18S* rRNA and are plotted as fold-change relative to the 0-minute point. Data are presented as mean + SEM, **P* < 0.05 vs. the 0-minute point as determined by 1-way ANOVA with Tukey's multiple-comparison test; *n* = 3 technical replicates/condition.

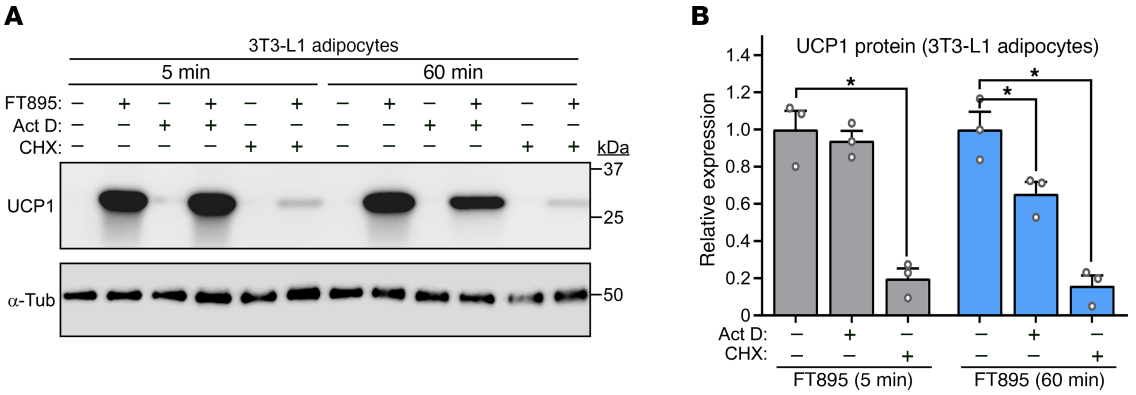


**Figure 4. HDAC11 inhibition promotes adipocyte UCP1 expression through posttranscriptional and transcriptional mechanisms.** (**A**) 3T3-L1 adipocytes were pretreated with vehicle (–), actinomycin D (Act D), or cycloheximide (CHX) for 30 minutes prior to exposure to FT895 for 5 or 60 minutes. Cells were homogenized and immunoblotting was performed. (**B**) Densitometric analysis of UCP1 expression in **A** as well as from 2 additional independent experiments (blots not shown), normalized to α-tubulin and plotted as fold-change relative to FT895 treatment alone. Data are presented as mean + SEM, with $^*P < 0.05$ as determined by 1-way ANOVA with Tukey's multiple-comparison test.

receptor desensitization, recent work has demonstrated that expression of the receptor is downregulated in response to chronic ligand exposure, nutrient excess, and/or inflammatory cues, leading to AT catecholamine resistance (27). Given the ability of HDAC11 inhibition to elicit UCP1 expression and PKA signaling independently of β-AR receptor ligand binding, experiments were performed to address the possibility that FT895 treatment circumvents $\beta_3$-AR downregulation in cell-based and in vivo models of catecholamine resistance. Initially, 3T3-L1 adipocytes were exposed to DMSO vehicle or the $\beta_3$-AR agonist CL-316,243 for 20 hours prior to 1 hour of reexposure to these agents, forskolin, which served as a positive control by virtue of its ability to stimulate adenylyl cyclase downstream of the receptor, or FT895 (Figure 8A). Consistent with prior findings, chronically treating adipocytes with CL-316,243 led to reduced $\beta_3$-AR protein expression and blocked subsequent UCP1 induction and PKA activation in response to acute reexposure to this agonist (Figure 8, B–D) (27). Strikingly, FT895 was as effective as forskolin at bypassing $\beta_3$-AR downregulation to stimulate UCP1 protein expression in adipocytes chronically treated with CL-316,243, and also promoted PKA signaling in these cells (Figure 8, B–D).

As an independent approach to determine whether HDAC11 inhibition can circumvent β-AR downregulation, 3T3-L1 adipocytes were infected with lentivirus expressing an shRNA targeting the *Adrb3* transcript, which encodes $\beta_3$-AR (Figure 8E). $\beta_3$-AR knockdown dramatically reduced CL-316,243–mediated UCP1 induction and PKA signaling, but did not substantially affect the ability of forskolin or FT895 to trigger these responses (Figure 8, F–H). Similar findings were observed when shRNA targeting $\beta_2$-AR was used, with knockdown of this receptor subtype blocking isoproterenol-induced (ISO-induced) UCP1 induction and PKA signaling, while having minimal effect on forskolin and FT895-mediated responses (Supplemental Figure 6, A–D). Of note, although ISO can stimulate all β-ARs, we have found that, at the concentration used in our experiments, this agonist predominantly promotes $\beta_2$-AR signaling in 3T3-L1 adipocytes (33).

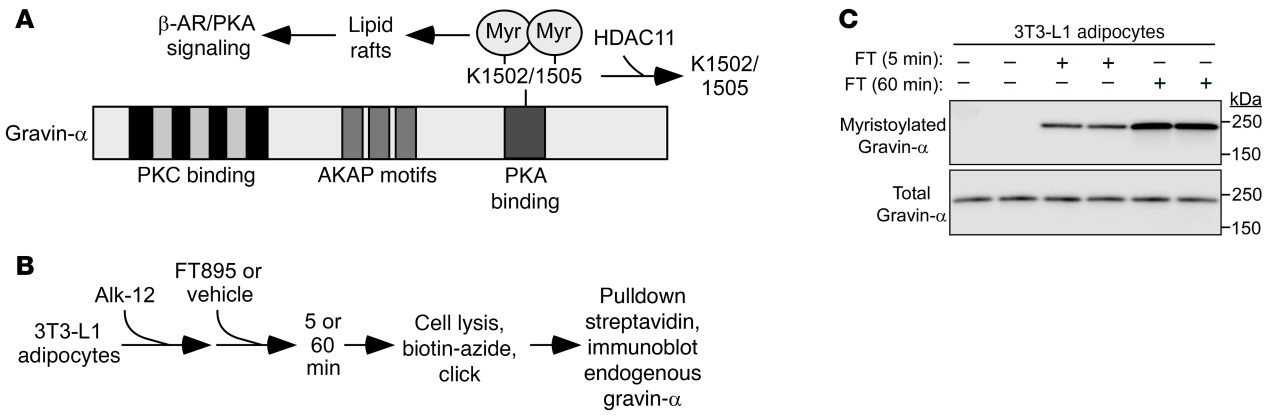


**Figure 5. HDAC11 inhibition promotes gravin-α myristoylation in adipocytes.** (**A**) Schematic representation of gravin-α protein structure, indicating the 2 lysine residues that are demyristoylated by HDAC11. Myristoylation of these 2 conserved lysines upon HDAC11 inhibition drives gravin-α:β-adrenergic receptor (β-AR) complexes into membrane lipid rafts, resulting in downstream protein kinase A (PKA) signaling. (**B**) Schematic depiction of the click chemistry experiment employing a myristic acid click tag (Alk-12) to determine whether acute HDAC11 inhibition with FT895 promotes gravin-α myristoylation. (**C**) Immunoblot analysis to detect endogenous myristoylated gravin-α and total gravin-α.

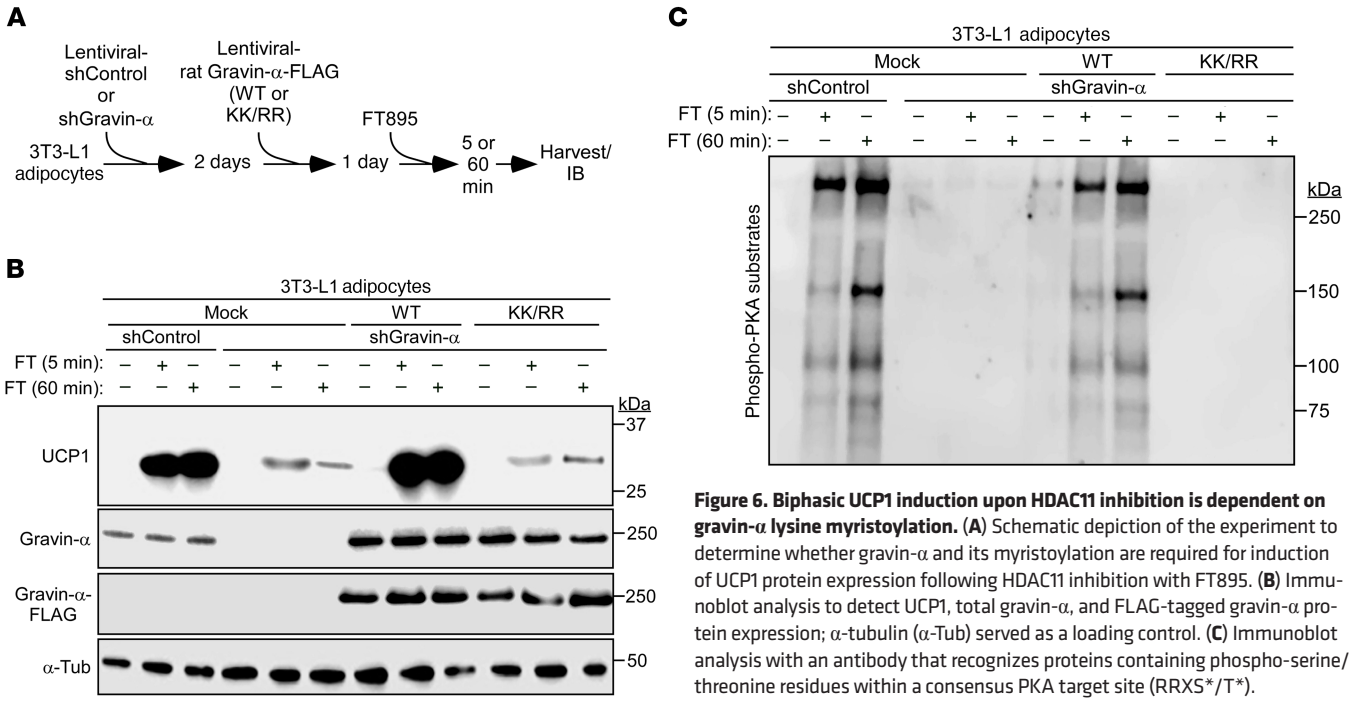


**Figure 6. Biphasic UCP1 induction upon HDAC11 inhibition is dependent on gravin-α lysine myristoylation.** (**A**) Schematic depiction of the experiment to determine whether gravin-α and its myristoylation are required for induction of UCP1 protein expression following HDAC11 inhibition with FT895. (**B**) Immunoblot analysis to detect UCP1, total gravin-α, and FLAG-tagged gravin-α protein expression; α-tubulin (α-Tub) served as a loading control. (**C**) Immunoblot analysis with an antibody that recognizes proteins containing phospho-serine/threonine residues within a consensus PKA target site (RRXS*/T*).

Signals emanating from the $\beta_3$-AR are transduced by the heterotrimeric G protein, $G_s$ (14). A third cell-based model of adipocyte catecholamine resistance took advantage of the fact that, while acute treatment of cells with cholera toxin (CTX) stimulates adenylyl cyclase by catalyzing ADP-ribosylation of the α subunit of the heterotrimeric G protein, Gαs, chronic exposure to the toxin leads to downregulation of Gαs expression by promoting its degradation (Supplemental Figure 6E) (34, 35). Since the $\beta_2$-AR also signals through Gαs, the CTX model enabled further assessment of the possible contribution of this GPCR to the ability of FT895 to bypass CL-316,243 resistance seen above. Exposure of 3T3-L1 adipocytes to CTX for 12 hours led to reduced Gαs abundance without influencing $\beta_3$-AR or $\beta_2$-AR expression (Supplemental Figure 6F). CTX pretreatment blocked subsequent UCP1 protein induction and PKA signaling following acute exposure of the cells to CL-316,243 or ISO (Supplemental Figure 6, F and G). Conversely, FT895 was still able to elicit these responses in cells treated with the toxin (Supplemental Figure 6, F and G). Thus, HDAC11 inhibition is capable of promoting UCP1 protein expression and PKA activation independently of β-AR signaling in 3 independent cell-based models of catecholamine resistance, 2 in which β-AR receptor expression is downregulated, and the other in which $\beta_2$- and $\beta_3$-AR coupling to Gαs is blocked.

In further support of β-AR–independent signaling events being triggered upon HDAC11 inhibition, treatment of 3T3-L1 adipocytes with the $\beta_3$-AR antagonist, L-748,337, or the $\beta_2$-AR antagonist, ICI-118,551, alone or in combination, failed to block FT895-mediated induction of UCP1 protein expression or PKA activation (Supplemental Figure 7, A–F). Parallel experiments with CL-316,243 and ISO confirmed that the antagonists, at the concentrations used, were effective at blocking adipocyte $\beta_3$-AR and $\beta_2$-AR signaling, respectively (Supplemental Figure 7, G and H).

To address the ability of HDAC11 inhibition to override AT catecholamine resistance in vivo, mice were injected with CL-316,243 or vehicle control for 12 hours prior to reexposure to these agents or treatment with FT895 for 1 additional hour (Figure 9A). Consistent with prior findings, CL-316,243 pretreatment led to a reduction in $\beta_3$-AR protein expression in eWAT, ingWAT, and BAT and blocked the subsequent induction of UCP1 protein and PKA signaling in each AT depot in response to acute reexposure to the agonist (Figure 9, B–E, and Supplemental Figure 8) (27). Strikingly, FT895 was effective even in the setting of catecholamine resistance in vivo, promoting UCP1 protein expression and PKA signaling in eWAT, ingWAT, and BAT of mice that were pretreated with CL-316,243 overnight (Figure 9, B–E, and Supplemental Figure 8, A–C).

*HDAC11 inhibition bypasses catecholamine resistance in human visceral adipose tissue ex vivo*. To further address the translational potential of inhibiting HDAC11, human visceral adipose tissue (VAT) explants from obese individuals undergoing bariatric surgery were treated with FT895 or vehicle control ex vivo. BODIPY staining confirmed the integrity of the explants (Figure 10A). FT895 treatment of human VAT for just 1 hour was sufficient to induce UCP1 protein expression, which was maintained for 20 hours following treatment (Figure 10B). Notably, FT895 stimulated UCP1 protein expression in human VAT as effectively as CL-316,243, isoproterenol, or forskolin (Figure 10C).

To assess whether HDAC11 inhibition is capable of promoting the thermogenic program in the setting of catecholamine resistance in human fat, VAT from 2 independent bariatric surgery patients was treated ex vivo with DMSO vehicle or CL-316,243 for 20 hours prior to reexposure to these agents or treatment with forskolin or FT895 for an additional 1 hour (Figure 10D). Chronic treatment with CL-316,243 led to reduced $\beta_3$-AR protein expression and blocked subsequent UCP1 protein induction and PKA activation following acute agonist exposure (Figure 10, E–G). Even

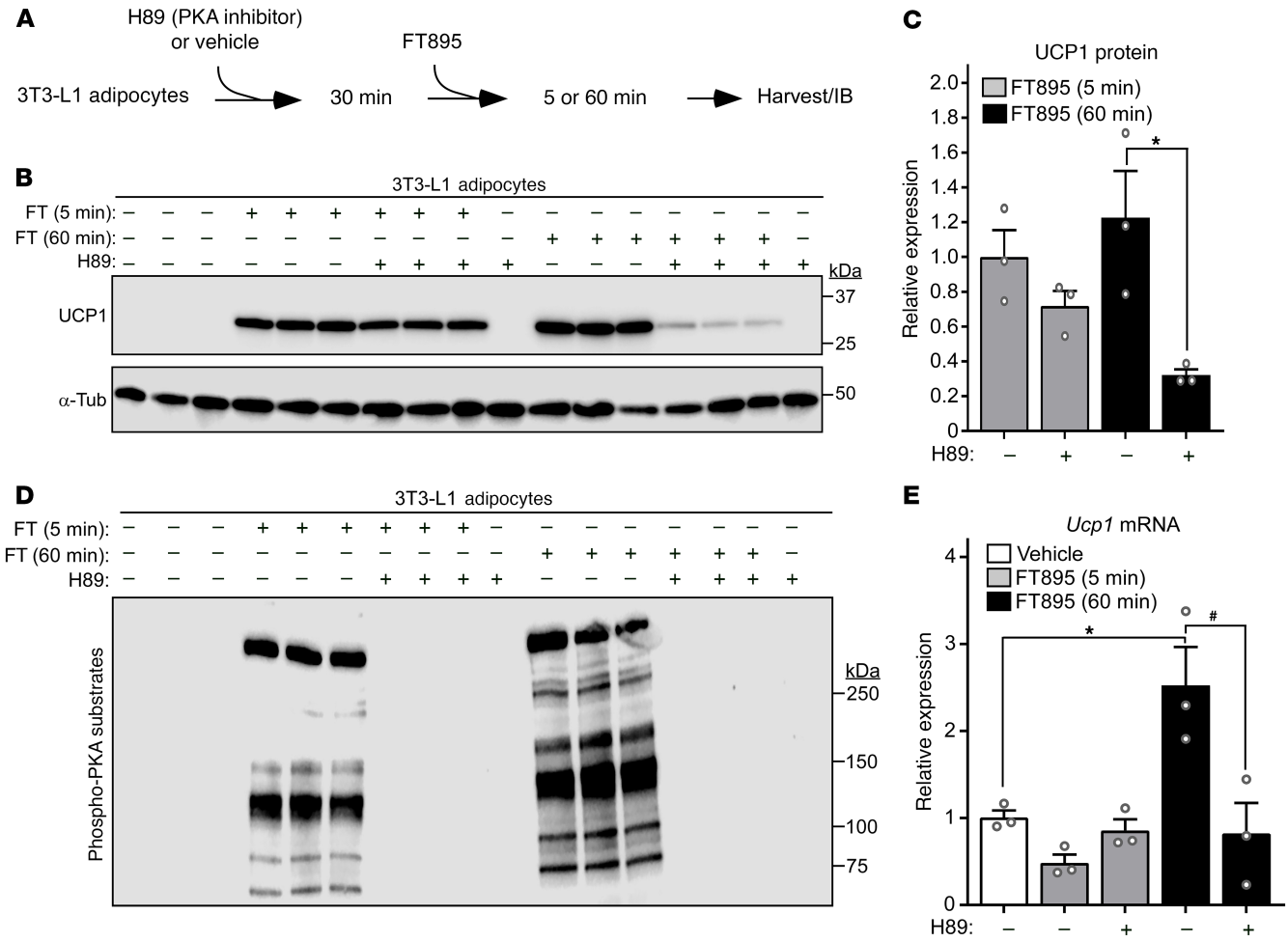


**Figure 7. Inhibition of HDAC11 stimulates PKA-independent and PKA-dependent induction of UCP1 expression.** (**A**) Schematic representation of the experiment to test the dependency of FT895-induced UCP1 expression on PKA signaling. (**B**) Immunoblot analysis of UCP1 protein expression, with α-tubulin (α-Tub) as a loading control; *n* = 3 technical replicates/condition. (**C**) Densitometric analysis of the UCP1 signal in **B**, normalized to α-Tub and depicted as fold-change relative to cells treated with FT895 alone. Data are presented as mean + SEM, with $^*P < 0.05$ as determined by 2-tailed, unpaired *t* test. (**D**) 3T3-L1 homogenates were immunoblotted with an antibody that recognizes proteins containing phospho-serine/threonine residues within a consensus PKA target site (RRXS*/T*). (**E**) *Ucp1* mRNA expression in 3T3-L1 adipocytes treated with FT895 for the indicated times in the absence or presence of H89 pretreatment was determined by qRT-PCR. Data were normalized to *18S* rRNA and are plotted as fold-change relative to the vehicle treated cells. Data are presented as mean + SEM, $^*P < 0.05$ vs. vehicle treatment and $^\#P < 0.05$ vs. 60-minute FT895 treatment without H89 as determined by 1-way ANOVA with Tukey's multiple-comparison test; *n* = 3 technical replicates/condition.

in obese human AT, FT895 was comparable to forskolin at circumventing $\beta_3$-AR downregulation to stimulate UCP1 protein expression and PKA signaling, underscoring the therapeutic potential of inhibiting HDAC11 in the context of adipocyte catecholamine resistance (Figure 10, E–G).

## Discussion

Attempts to stimulate BAT and beiging of WAT in humans using $\beta_3$-AR agonists have met with only limited success, perhaps due to $\beta_3$-AR downregulation in response to chronic ligand exposure and/or metabolic disease–induced inflammation, processes referred to as homologous and heterologous receptor desensitization, respectively (27). Here, we provide rationale for employing selective HDAC11 inhibitors to modulate AT phenotype independently of $\beta_3$-AR agonism. Adipocyte-specific deletion or pharmacological inhibition of HDAC11 with FT895 potently drives UCP1 expression and PKA signaling in BAT and WAT, even when the $\beta_3$-AR is desensitized due to prolonged agonist treatment or CTX-mediated Gαs degradation. Furthermore, FT895 is capable of stimulating UCP1 and PKA in adipocytes in which $\beta_3$- and $\beta_2$-AR expression is knocked down with shRNA, and in cells treated with β-AR antagonists. HDAC11 inhibition triggers ultrarapid, posttranscriptional induction of UCP1 protein expression that occurs independently of PKA signaling, and also delayed induction of UCP1 expression that is governed by PKA and requires de novo mRNA synthesis (Figure 10H). We posit that this biphasic mechanism enables efficient thermogenic adaptation to acute and chronic environmental stress.

Stimulation of UCP1 expression in adipocytes following HDAC11 inhibitor treatment was dependent on site-specific myristoylation of gravin-α. Gravin-α is a scaffolding protein that harbors distinct binding domains for multiple proteins, including PKA

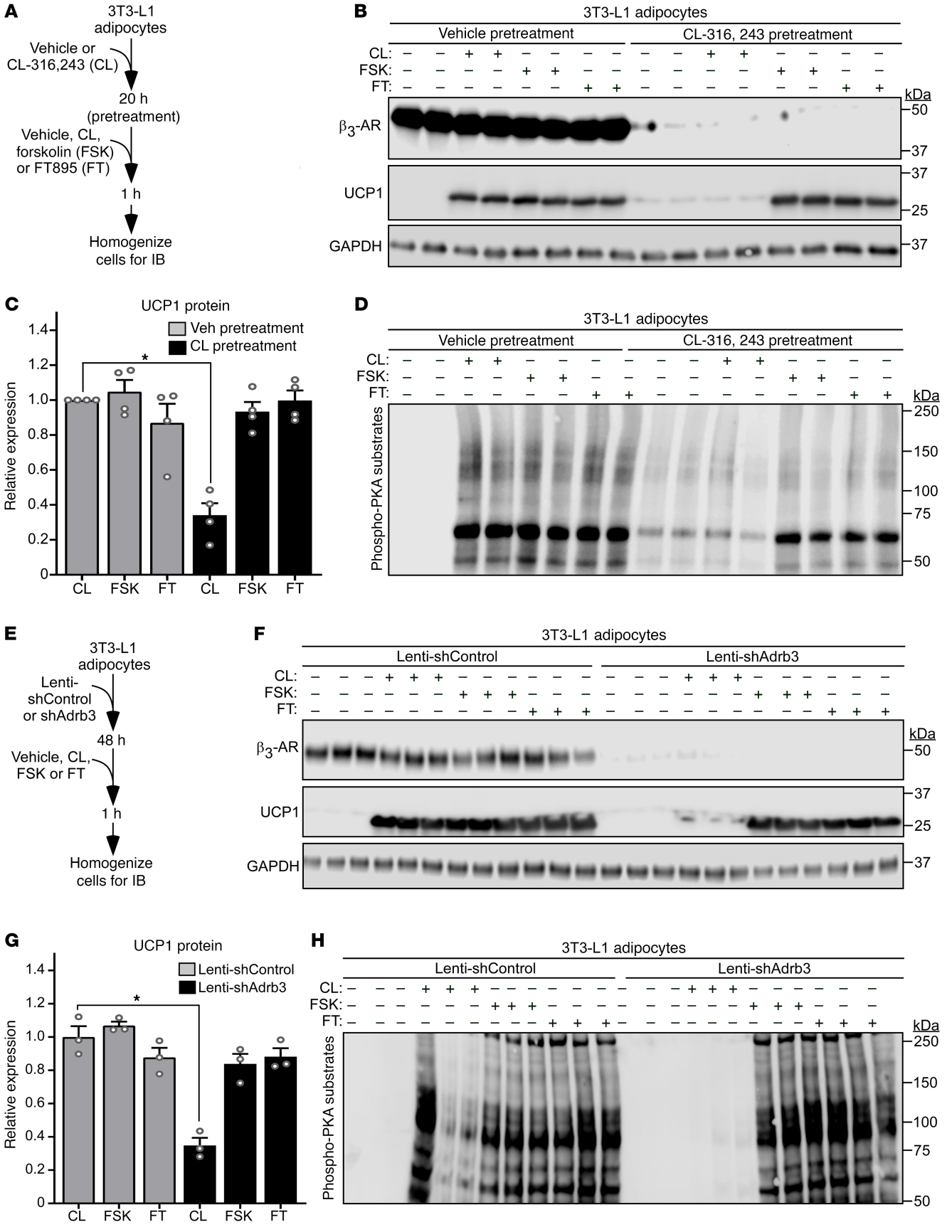
A
3T3-L1 adipocytes
Vehicle or CL-316,243 (CL)
20 h (pretreatment)
Vehicle, CL, forskolin (FSK) or FT895 (FT)
1 h
Homogenize cells for IB
B
3T3-L1 adipocytes
Vehicle pretreatment
CL-316, 243 pretreatment
CL:
FSK:
FT:
kDa
β3-AR
UCP1
GAPDH
50
37
25
C
UCP1 protein
Veh pretreatment
CL pretreatment
Relative expression
CL FSK FT CL FSK FT
D
3T3-L1 adipocytes
Vehicle pretreatment
CL-316, 243 pretreatment
Phospho-PKA substrates
250
150
100
75
50
E
3T3-L1 adipocytes
Lenti-shControl or shAdrb3
48 h
Vehicle, CL, FSK or FT
1 h
Homogenize cells for IB
F
3T3-L1 adipocytes
Lenti-shControl
Lenti-shAdrb3
G
UCP1 protein
Lenti-shControl
Lenti-shAdrb3
H
3T3-L1 adipocytes
Lenti-shControl
Lenti-shAdrb3

**Figure 8. HDAC11 inhibition promotes UCP1 expression and PKA signaling in cell-based models of catecholamine resistance.** (**A**) Schematic representation of the cell culture experiment to determine whether HDAC11 inhibition promotes adipocyte UCP1 expression and PKA signaling in the context of downregulated $\beta_3$-adrenergic receptor ($\beta_3$-AR) expression due to chronic agonist exposure. (**B**) Immunoblot analysis of 3T3-L1 cells pretreated with vehicle or the $\beta_3$-AR agonist CL-316,243 (CL) for 20 hours followed by 1-hour treatment with vehicle (–), CL, the adenylyl cyclase activator forskolin (FSK), or FT895; *n* = 2 technical replicates/condition. (**C**) Densitometric analysis of UCP1 expression in **B**, and from 2 additional independent experiments (blots not shown), normalized to GAPDH and plotted as fold-change relative to CL treatment alone. Expression of UCP1 with vehicle pretreatment + CL is set to 1 within each independent experiment. Data are presented as mean + SEM, with $*P < 0.05$ as determined by 1-way ANOVA with Tukey's multiple-comparison test. (**D**) These same samples were independently immunoblotted with an antibody that recognizes proteins containing phospho-serine/threonine residues within a consensus PKA target site (RRXS*/T*). (**E**) Schematic representation of the cell culture experiment to determine whether HDAC11 inhibition promotes adipocyte UCP1 expression and PKA signaling in the context of catecholamine resistance due to knockdown of $\beta_3$-AR expression. (**F**) Immunoblot analysis of the indicated proteins in homogenates of 3T3-L1 cells; *n* = 3 technical replicates/condition. (**G**) Densitometric analysis of UCP1 expression in **F** normalized to GAPDH and plotted as fold-change relative to Lenti-shAdrb3 + CL. Data are presented as mean + SEM, with $*P < 0.05$ determined by 1-way ANOVA with Tukey's multiple-comparison test. (**H**) Immunoblot analysis with the anti–phospho-PKA-substrate antibody.

and $\beta_2$- and $\beta_3$-ARs (33, 36–38). Previously, we showed that, upon HDAC11 inhibition, gravin-α is myristoylated on lysines 1502 and 1505, which leads to translocation of gravin-α:$\beta_3$-AR:PKA protein complexes to plasma membrane lipid rafts containing proteins such as caveolin-1 and flotillin-2 (33). Targeting of the $\beta_3$-AR to lipid rafts is required to efficiently trigger downstream PKA signaling and UCP1 induction in response to receptor ligands. The ability of FT895 to elicit these effects in the context of catecholamine resistance suggests that simply targeting gravin-α to lipid rafts is sufficient to promote downstream signaling, even in the absence of $\beta_3$-AR engagement and Gs coupling. The mechanism(s) underlying such receptor-independent signaling mediated by myristoylated gravin-α remains unknown. FT895 treatment did not alter binding of PKA subunits to gravin-α. However, it remains possible that HDAC11 inhibition promotes recruitment of gravin-α–bound PKA to cyclic AMP–rich (cAMP-rich) regions juxtaposing the cell membrane, or triggers lipid raft–dependent changes in the association of gravin-α with other effector proteins. We also cannot rule out the possibility that myristoylated gravin-α promotes adenylyl cyclase activity or alters phosphodiesterase function. In this regard, it is noteworthy that, at the level of phospho-PKA-substrate immunoblotting, FT895 treatment elicited a pattern of protein phosphorylation that was qualitatively similar to that induced by forskolin or β-AR agonists. As an extension of our findings with adipocytes, it will be important to determine whether HDAC11 inhibition is sufficient to stimulate PKA signaling in other catecholamine-responsive cell types, such as cardiomyocytes and smooth muscle cells.

The PKA-independent, gravin-α–dependent mechanism(s) for acute induction of UCP1 protein expression following FT895 treatment remains to be defined, but likely involves lipid raft–mediated activation of another gravin-α–associated signaling effector. While we are unaware of other demonstrations of a robust increase in UCP1 protein expression after 5 minutes of exposure to a stimulus, prior work illustrated a UCP1-dependent elevation of mouse BAT temperature within 2–3 minutes following administration of CL-316,243 in vivo, which is consistent with a role for posttranscriptional induction of UCP1 in acute adaptation to stress (39). Posttranscriptional mechanisms for regulating UCP1 protein expression independently of changes in *Ucp1* mRNA abundance have been described, and include translational control via binding of polyadenylation element–binding protein 2 (CPEB2) and insulin-like growth factor 2 mRNA-binding protein 2 (IGF2BP2) to untranslated regions (UTRs) of the *Ucp1* transcript (40, 41). Thus, it is possible that FT895-mediated activation of gravin-α signaling promotes acute UCP1 protein synthesis by modulating the activity of UTR-binding proteins.

Transcriptional regulation of the *Ucp1* gene has been studied in detail and involves binding of transcription factors such as cAMP response element–binding protein (CREB), activating transcription factor 2 (ATF-2), and peroxisome proliferator-activated receptor γ (PPARγ) to upstream distal enhancer and proximal promoter regions of the gene (42). PKA regulates *Ucp1* gene expression, in part, by simulating p38 mitogen–activated protein kinase, which phosphorylates ATF2 and PPARγ coactivator 1α (PGC-1α), priming these proteins to bind to conserved cAMP- and PPAR-associated response elements in the *Ucp1* enhancer region, respectively (43). Induction of adipocyte UCP1 protein expression following chronic treatment with FT895 presumably involves PKA-dependent activation of this signaling and transcription factor axis.

The *Ucp1* gene is also subject to active repression, such as through the action of nuclear receptor–interacting protein 1 (NRIP1) (44). Additionally, we previously demonstrated that a nuclear pool of HDAC11 interacts with the chromatin reader protein, BRD2, to suppress *Ucp1* gene expression (31). In this regard, it is noteworthy that FT895 failed to stimulate UCP1 expression in adipocytes in which gravin-α was knocked down, which was unexpected since the pharmacological inhibitor should engage BRD2-bound HDAC11 independently of the scaffolding protein. This finding suggests that inhibition of nuclear HDAC11 is necessary but not sufficient to induce UCP1 expression. We posit that in adipocytes chronically treated with FT895, gravin-α–dependent stimulation of PKA/p38 signaling provides a second hit by activating transcription factors (e.g., ATF2 and PPARγ), which work in concert with inhibition of nuclear HDAC11 to promote *Ucp1* mRNA synthesis.

Surprisingly, deletion or pharmacological inhibition of HDAC11 in preadipocytes also led to biphasic, PKA-independent and PKA-dependent UCP1 induction. Although uncommon, there are other examples of UCP1 expression in adipocyte precursor cells. Fibroblast growth factors 6 and 9 (FGF6/9) were found to function as adipokines with the capacity to stimulate UCP1 expression in preadipocytes (45). Upregulation of UCP1 by FGF6/9 occurred independently of canonical transcriptional mediators of thermogenesis such as PPARγ, and instead required a complex containing the nuclear hormone receptor, estrogen-related receptor-α. In a separate study, ectopic expression of the AT-enriched transcriptional coactivator, regulator PR domain containing 16 (PRDM16), in combination

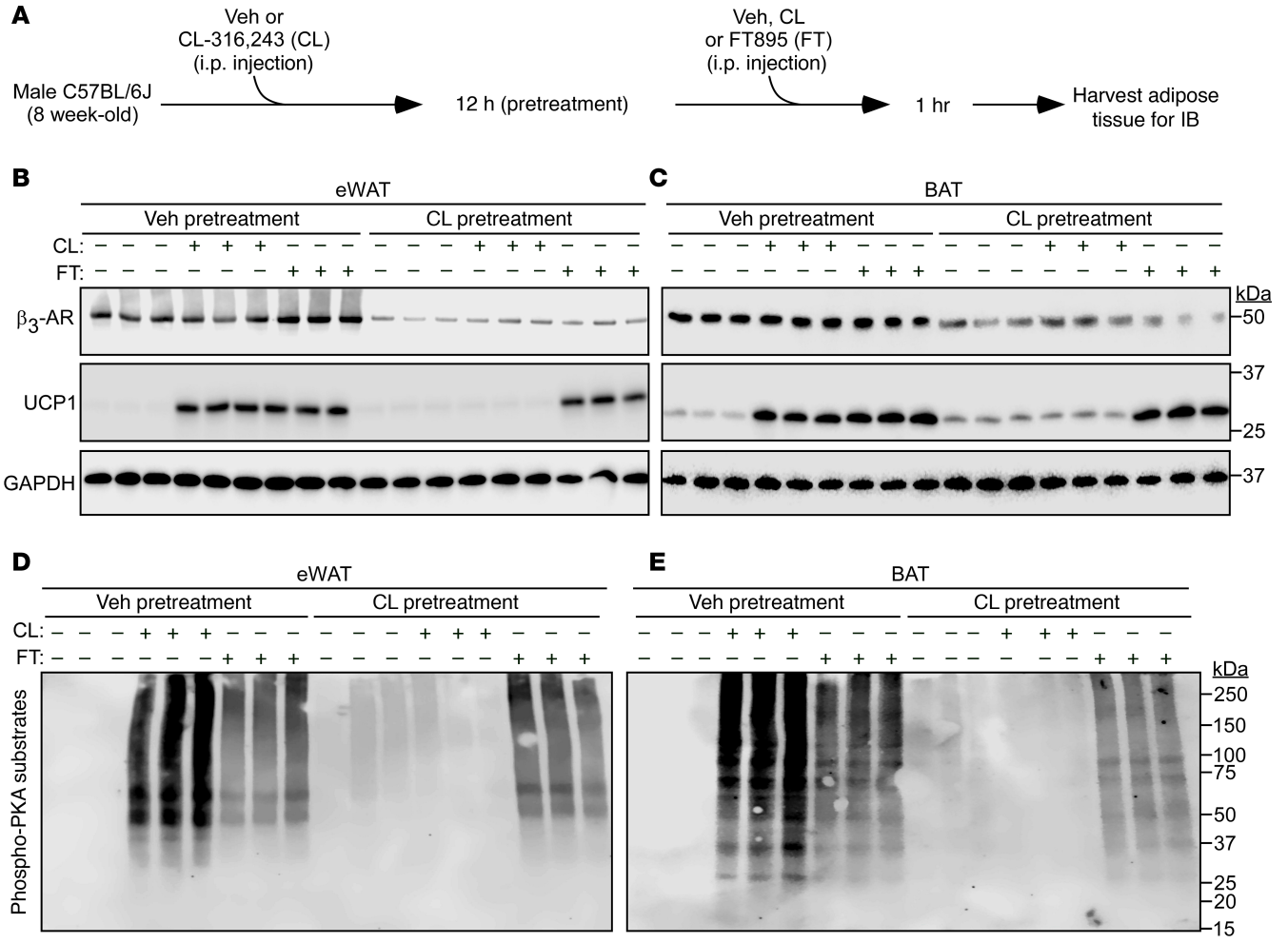


**Figure 9. HDAC11 inhibition bypasses adipose tissue catecholamine resistance in vivo.** (**A**) Schematic representation of the in vivo experiment to determine whether HDAC11 inhibition promotes UCP1 expression and PKA signaling in the context of downregulated $\beta_3$-adrenergic receptor ($\beta_3$-AR) expression in adipose tissue. (**B** and **C**) Immunoblot analysis of the indicated proteins in homogenates of epididymal white adipose tissue (eWAT) and interscapular brown adipose tissue (BAT) in mice pretreated with vehicle (Veh) or CL-316,243 (CL) for 12 hours followed by 1-hour treatment with vehicle (–), CL, or FT895 (FT); *n* = 3 biological replicates/condition. (**D** and **E**) These same samples were independently immunoblotted with an antibody that recognizes proteins containing phospho-serine/threonine residues within a consensus PKA target site (RRXS*/T*).

with forskolin treatment, was demonstrated to promote *Ucp1* mRNA expression in mouse embryonic fibroblasts (MEFs) (46). PRDM16-mediated expression of *Ucp1* expression in MEFs was in part dependent on stimulation of the transcriptional activity of another nuclear hormone receptor, thyroid hormone receptor. Whether HDAC11 inhibition activates either of the nuclear hormone receptor transcriptional pathways to promote UCP1 expression in preadipocytes remains to be determined.

Combining an HDAC11 inhibitor with existing antiobesity drugs has the potential to enhance efficacy and improve the therapeutic index of these agents by directly altering AT phenotype. In this regard, our preliminary studies revealed reduced weight gain and fat mass in $Hd11^{cKO}$ mice fed HFD for 16 weeks compared with controls. There are 4 FDA-approved HDAC inhibitors for the treatment of hematologic tumors, establishing the viability of targeting this class of enzymes to treat human diseases (47). Nonetheless, these general HDAC inhibitors are poorly tolerated at the relatively high doses required to block tumor growth, and thus there is great interest in developing isoform-selective HDAC inhibitors with the goal of improving tolerability and efficacy. The discovery of FT895, which is more than 1,500-fold selective for HDAC11 over the other 10 zinc-dependent HDACs, has established the feasibility of selectively inhibiting this enzyme with a pharmacological agent (48). However, while FT895 is an excellent tool for research, it lacks oral bioavailability and harbors a hydroxamic acid warhead, which has been linked to mutagenicity in other compounds (48, 49). Thus, future clinical development of HDAC11 inhibitors will require additional medicinal chemistry efforts to overcome these liabilities while maintaining selectivity and potency for this HDAC isoform.

In conclusion, we have shown that HDAC11 inhibition is as effective as $\beta_3$-AR stimulation or direct adenylyl cyclase activation at stimulating UCP1 protein expression in murine and human AT. HDAC11 functions in an adipocyte-autonomous manner to control thermogenesis, as opposed to altering the phenotype of fat via indirect mechanisms such as by regulating adrenergic drive.

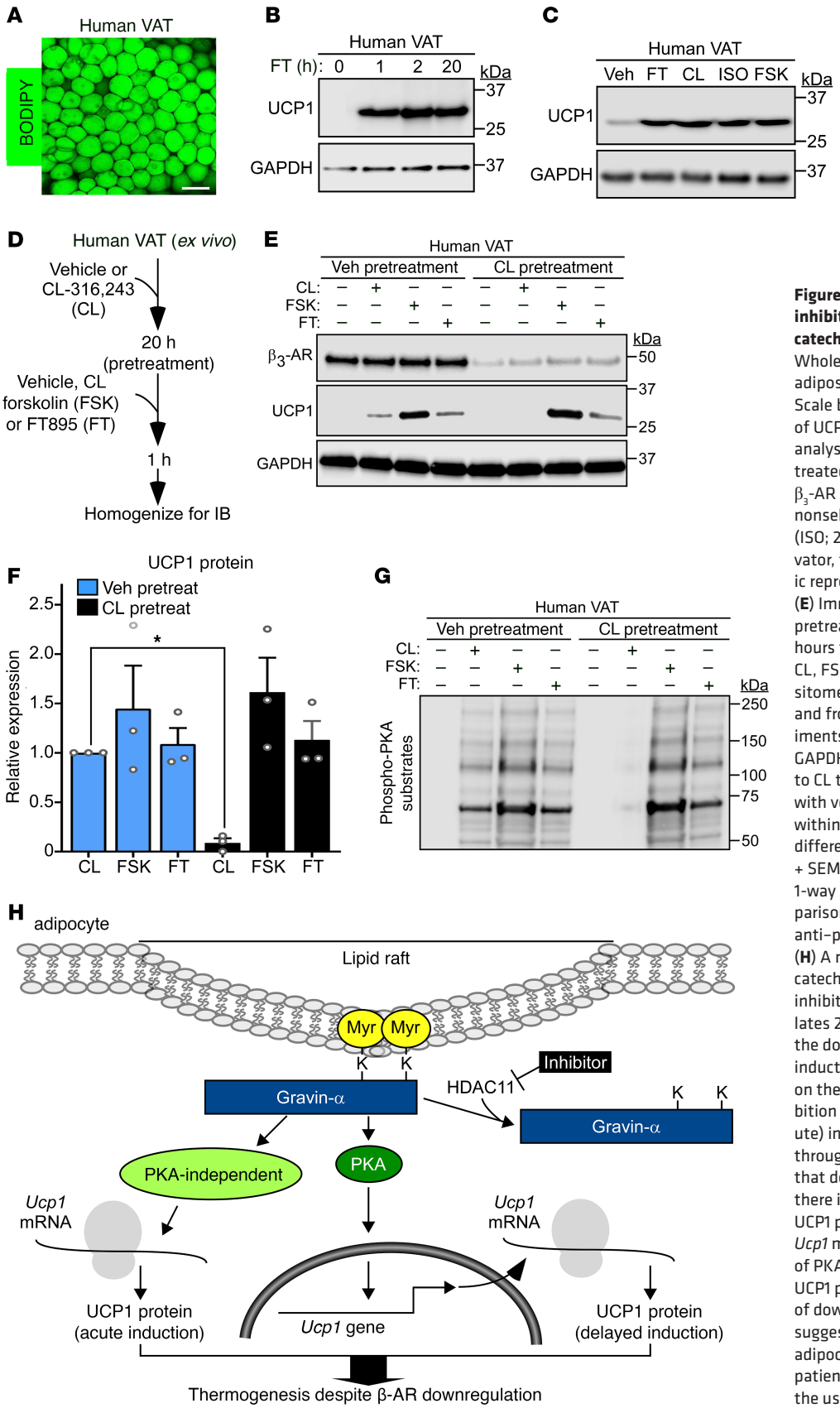


**Figure 10. Therapeutic potential of inhibiting HDAC11 to circumvent adipocyte catecholamine resistance in humans.** (**A**) Whole-mount image of human visceral adipose tissue (VAT) stained with BODIPY. Scale bar: 100 μm. (**B**) Immunoblot analysis of UCP1 and GAPDH. (**C**) Immunoblot analysis of UCP1 and GAPDH in human VAT treated ex vivo with FT895 (FT; 1 hour); the $\beta_3$-AR agonist, CL-316,243 (CL; 3 hours); the nonselective β-AR agonist, isoproterenol (ISO; 2 hours); or the adenylyl cyclase activator, forskolin (FSK; 2 hours). (**D**) Schematic representation of the ex vivo experiment. (**E**) Immunoblot analysis of human VAT pretreated ex vivo with vehicle or CL for 20 hours followed by exposure to vehicle (–), CL, FSK, or FT for 1 additional hour. (**F**) Densitometric analysis of UCP1 expression in **E**, and from 2 additional independent experiments (blots not shown), normalized to GAPDH and plotted as fold-change relative to CL treatment alone. Expression of UCP1 with vehicle pretreatment + CL is set to 1 within each independent experiment; $n = 3$ different patient samples/condition. Mean + SEM, with $^*P < 0.05$, as determined by 1-way ANOVA with Tukey's multiple-comparison test. (**G**) Immunoblotting with the anti–phospho-PKA substrate antibody. (**H**) A model for circumventing adipocyte catecholamine resistance through HDAC11 inhibition. HDAC11 normally demyristoylates 2 lysine residues in gravin-α, blocking the downstream signaling needed for UCP1 induction. When gravin-α is myristoylated on these lysines, such as upon HDAC11 inhibition with FT895, there is acute (5-minute) induction of UCP1 protein expression through a posttranscriptional mechanism that does not require PKA signaling, and there is delayed (60-minute) induction of UCP1 protein expression that requires new *Ucp1* mRNA synthesis and is dependent of PKA signaling. HDAC11 inhibition drives UCP1 protein expression even in the context of downregulated β-adrenergic receptors, suggesting the possibility of overcoming adipocyte catecholamine resistance in patients with metabolic disease through the use of HDAC11 inhibitors.

HDAC11 inhibition triggers UCP1 expression through posttranscriptional and transcriptional mechanisms, both of which require site-specific myristoylation of gravin-α. The ability of HDAC11 inhibition to function in a β-AR–independent manner to bypass AT catecholamine resistance underscores the potential of targeting this lysine demyristoylase as a therapeutic strategy for metabolic diseases that have been recalcitrant to $\beta_3$-AR agonists.

## Methods

Further information can be found in Supplemental Methods.

*Creation of Hd11$^{cKO}$ mice*. CRISPOR and the Broad Institute sgRNA Design software were used to design guide RNAs (50, 51). Guides that performed best by both software programs were selected, and guide activity was verified by incubating sgRNA and Cas9 protein with a PCR product containing the target sequence and comparing the ratio of cut to uncut PCR product. Zygotes were injected with an sgRNA (Synthego) with target sequence + PAM CAAGGCCCAAGGCCTGCACG + GGG, Cas9 protein (Integrated DNA Technologies, Alt-R *Streptococcus pyogenes* HiFi Cas9 Nuclease V3), and single-stranded DNA template (Integrated DNA Technologies), starting with the weaker guide. Zygotes were then transferred into pseudopregnant recipients. $F_0$ pups were genotyped by PCR using primers outside the region to be modified to identify putative positive founders; PCR primer sequences are provided in Supplemental Table 1. These mice were then bred with appropriate WT mice. $F_1$ male pups were genotyped and sequence confirmed for the desired introduction of a lone *loxP* site. $F_1$ males were then used as sperm donors for IVF with B6N WT eggs and resulting zygotes were microinjected with a second sgRNA with target sequence + PAM of CTCGGGGGACCTCCTATCTA + CGG, Cas9 protein, and a second DNA template to introduce the second *loxP* site. $F_0$ mice were genotyped for both mutations. Mice with both *loxP* sites were bred with WT B6N mice. Cosegregation of the *loxP* sites indicates that they are in *cis*, indicative of a floxed allele. Once homozygous (*Hdac11$^{fl/fl}$*) mice were generated, both *loxP* sites were again sequenced via Sanger sequencing using primers outside of the DNA template sequence to verify the integration of fully intact *loxP* sites. *Hdac11$^{fl}$* mice were crossed with *Adipoq-Cre* mice purchased from the Jackson Laboratory (stock 028020). *Hdac11$^{fl/fl}$* mice were generated in the Regional Mouse Genetics Core Facility, which is supported by both National Jewish Health and the University of Colorado Anschutz Medical Campus.

*Cold challenge and HFD feeding*. All chemicals and reagents used for the current studies are described in Supplemental Table 2. Patient demographics are provided in Supplemental Tables 3 and 4, and antibodies are indicated in Supplemental Table 5. Antibody validation data are provided in Supplemental Figure 9. Mice were housed singly for 5 days prior to commencement of the 24-hour 4°C challenge. Core body temperature was monitored at the indicated times for the duration of the study using a rectal probe (Physitemp Instruments Inc.) connected to a physiological monitoring unit (THM150, VisualSonics). WT C57BL/6J mice (Jackson Laboratory, stock 000664) were employed for the 4°C studies with FT895. FT895 was delivered in a vehicle of 5% DMA/1% Tween 80/94% sterile water by i.p. injection for the 5 days of thermoneutral acclimatization and for the duration of the experiment. All 4°C challenge experiments were performed within the University of Colorado Nutrition and Obesity Center (NORC) small animal Energy Balance Assessment core.

Ten- to 12-week-old male mice were fed an HFD (Research Diets Inc., D09071702; 58% calories derived from fat) or normal chow for 16 weeks. Body composition was determined using MRI (EchoMRI) to assess fat and lean absolute and percentage mass. Glucose tolerance was determined in mice that were fasted overnight prior to administration of glucose (2 mg/g body weight) via intraperitoneal (i.p.) injection. Tail vein blood was collected and blood glucose measured using a commercial glucometer (Bayer Contour) at baseline and at 15, 30, 60, 90, and 120 minutes after glucose administration.

*In vivo model of catecholamine resistance*. The in vivo procedure to downregulate $\beta_3$-AR expression in AT has been described previously (27). Briefly, 8-week-old male WT mice (Jackson Laboratory, stock 000664) were pretreated with an i.p. injection of CL-316,243 (0.5 mg/kg in sterile saline) or vehicle only of the same volume. After 12 hours, a second dose of CL-316,243 (0.1 mg/kg) or FT895 (10 mg/kg in 5% DMA/1% Tween 80/94% sterile water) or vehicle (5% DMA/1% Tween 80/94% sterile water) was administered by i.p. injection, and after 1 subsequent hour, animals were euthanized and tissues harvested. Throughout the experiment, mice were given ad libitum access to chow and water.

*Statistics*. All data are presented as mean + SEM. Statistical significance was determined using unpaired, 2-tailed *t* test (2 groups) or 1-way ANOVA with correction for multiple comparisons via Tukey's post hoc test (GraphPad Prism 9) unless otherwise specified. A *P* value of less than 0.05 was considered statistically significant.

*Study approval*. All animal studies were conducted using a protocol approved by the Institutional Animal Care and Use Committee of the University of Colorado Anschutz Medical Campus, following appropriate guidelines and in accordance with the NIH *Guide for the Care and Use of Laboratory Animals* (National Academies Press, 2011).

Human VAT samples were acquired from bariatric surgery patients under protocols approved by Colorado Multiple Institutional Review Board.

*Data availability*. Data for graphs are provided in the Supporting Data Values Excel file. See complete unedited immunoblots in the supplemental material.

## Author contributions

ELR, RAB, JL Major, and TAM conceived and designed the study. ELR, RAB, and JL Major acquired data. ELR, RAB, JL Major, JL Matsuda, and TAM analyzed and interpreted data. ELR, RAB, JL Major, BCB, JL Matsuda, and TAM wrote and reviewed the manuscript. BCB and JL Matsuda provided administrative, technical, or material support. TAM supervised the study. The order of the first or last authors reflects the leadership exerted in the study.

## Acknowledgments

The authors wish to acknowledge the Regional Mouse Genetics Core Facility, which is supported by both National Jewish Health and the University of Colorado Anschutz Medical Campus. Metabolic phenotyping studies were performed in the Colorado Nutrition Obesity Research Center (NORC) Animal Satellite Facility (supported by NIDDK grant DK048520). We thank K.M. Gavin for human subcutaneous adipocyte isolation, E. Seto for the HDAC11 antibody, J. Miano for the rat gravin-α cDNA construct, T. Hu for cloning, and J.G. Travers for critical review of the manuscript. ELR was funded by the American Heart Association (grant 829504), and RAB and JL Major received support from the Canadian Institutes

of Health Research (grants FRN-216927 and FRN-395620, respectively). RAB is currently supported by a Career Development Award from the American Heart Association (23CDA1048663), Sturgis Endowment Grant for Diabetes Research, and Brunson Pilot Award for Cardiovascular Research (UAMS). TAM received funding from NIH grants HL116848, HL147558, DK119594, HL127240, and HL150225, and a grant from the American Heart Association (16SFRN31400013). The contents are the authors' sole responsibility and do not necessarily represent official NIH views.

Address correspondence to: Department of Medicine, Division of Cardiology, University of Colorado Anschutz Medical Campus, RC2, Room 8014A, Mail Stop B139, 12700 E. 19th Ave, Aurora, Colorado 80045-2507, USA. Phone: 303.724.5476; Email: timothy.mckinsey@cuanschutz.edu.

RAB's present address is: Department of Internal Medicine, Division of Cardiovascular Medicine, University of Arkansas for Medical Sciences, Little Rock, Arkansas, USA.

1. Hales CM, et al. Prevalence of obesity among adults and youth: United States, 2015-2016. *NCHS Data Brief*. 2017;(288):1–8.
2. Hales CM, et al. Prevalence of obesity and severe obesity among adults: United States, 2017-2018. *NCHS Data Brief*. 2020;(360):1–8.
3. Drucker DJ. GLP-1 physiology informs the pharmacotherapy of obesity. *Mol Metab*. 2022;57:101351.
4. Kusminski CM, et al. Targeting adipose tissue in the treatment of obesity-associated diabetes. *Nat Rev Drug Discov*. 2016;15(9):639–660.
5. Pfeifer A, Hoffmann LS. Brown, beige, and white: the new color code of fat and its pharmacological implications. *Annu Rev Pharmacol Toxicol*. 2015;55:207–227.
6. Cannon B, et al. Brown adipose tissue. More than an effector of thermogenesis? *Ann N Y Acad Sci*. 1998;856:171–187.
7. Fedorenko A, et al. Mechanism of fatty-acid-dependent UCP1 uncoupling in brown fat mitochondria. *Cell*. 2012;151(2):400–413.
8. Nicholls DG, et al. The identification of the component in the inner membrane of brown adipose tissue mitochondria responsible for regulating energy dissipation. *Experientia Suppl*. 1978;32:89–93.
9. Rosen ED, Spiegelman BM. What we talk about when we talk about fat. *Cell*. 2014;156(1–2):20–44.
10. Cypess AM, et al. Identification and importance of brown adipose tissue in adult humans. *N Engl J Med*. 2009;360(15):1509–1517.
11. Nedergaard J, et al. Unexpected evidence for active brown adipose tissue in adult humans. *Am J Physiol Endocrinol Metab*. 2007;293(2):E444–E452.
12. van Marken Lichtenbelt WD, et al. Cold-activated brown adipose tissue in healthy men. *N Engl J Med*. 2009;360(15):1500–1508.
13. Virtanen KA, et al. Functional brown adipose tissue in healthy adults. *N Engl J Med*. 2009;360(15):1518–1525.
14. Collins S. β-Adrenergic receptors and adipose tissue metabolism: evolution of an old story. *Annu Rev Physiol*. 2022;84:1–16.
15. Arch JR. Challenges in β(3)-adrenoceptor agonist drug development. *Ther Adv Endocrinol Metab*. 2011;2(2):59–64.
16. Larsen TM, et al. Effect of a 28-d treatment with L-796568, a novel beta(3)-adrenergic receptor agonist, on energy expenditure and body composition in obese men. *Am J Clin Nutr*. 2002;76(4):780–788.
17. van Baak MA, et al. Acute effect of L-796568, a novel beta 3-adrenergic receptor agonist, on energy expenditure in obese men. *Clin Pharmacol Ther*. 2002;71(4):272–279.
18. Weyer C, et al. , and Ravussin E. Increase in insulin action and fat oxidation after treatment with CL 316,243, a highly selective beta3-adrenoceptor agonist in humans. *Diabetes*. 1998;47(10):1555–1561.
19. Baskin AS, et al. Regulation of human adipose tissue activation, gallbladder size, and bile acid metabolism by a β3-adrenergic receptor agonist. *Diabetes*. 2018;67(10):2113–2125.
20. Blondin DP, et al. Human brown adipocyte thermogenesis is driven by β2-AR stimulation. *Cell Metab*. 2020;32(2):287–300.
21. Cypess AM, et al. Activation of human brown adipose tissue by a β3-adrenergic receptor agonist. *Cell Metab*. 2015;21(1):33–38.
22. Loh RKC, et al. Acute metabolic and cardiovascular effects of mirabegron in healthy individuals. *Diabetes Obes Metab*. 2019;21(2):276–284.
23. Finlin BS, et al. The β3-adrenergic receptor agonist mirabegron improves glucose homeostasis in obese humans. *J Clin Invest*. 2020;130(5):2319–2331.
24. Flier JS. Might β3-adrenergic receptor agonists be useful in disorders of glucose homeostasis? *J Clin Invest*. 2020;130(5):2180–2182.
25. O'Mara AE, et al. Chronic mirabegron treatment increases human brown fat, HDL cholesterol, and insulin sensitivity. *J Clin Invest*. 2020;130(5):2209–2219.
26. Riis-Vestergaard MJ, et al. Beta-1 and not beta-3 adrenergic receptors may be the primary regulator of human brown adipocyte metabolism. *J Clin Endocrinol Metab*. 2020;105(4):dgz298.
27. Valentine JM, et al. β3-Adrenergic receptor downregulation leads to adipocyte catecholamine resistance in obesity. *J Clin Invest*. 2022;132(2):e153357.
28. Cao J, et al. HDAC11 regulates type I interferon signaling through defatty-acylation of SHMT2. *Proc Natl Acad Sci U S A*. 2019;116(12):5487–5492.
29. Kutil Z, et al. Histone deacetylase 11 is a fatty-acid deacylase. *ACS Chem Biol*. 2018;13(3):685–693.
30. Moreno-Yruela C, et al. Histone deacetylase 11 is an ε-N-myristoyllysine hydrolase. *Cell Chem Biol*. 2018;25(7):849–856.e8.
31. Bagchi RA, et al. HDAC11 suppresses the thermogenic program of adipose tissue via BRD2. *JCI Insight*. 2018;3(15):e120159.
32. Sun L, et al. Programming and regulation of metabolic homeostasis by HDAC11. *EBioMedicine*. 2018;33:157–168.
33. Bagchi RA, et al. Reversible lysine fatty acylation of an anchoring protein mediates adipocyte adrenergic signaling. *Proc Natl Acad Sci U S A*. 2022;119(7):e2119678119.
34. Chang FH, Bourne HR. Cholera toxin induces cAMP-independent degradation of Gs. *J Biol Chem*. 1989;264(10):5352–5357.
35. Milligan G, et al. Cholera toxin treatment produces down-regulation of the alpha-subunit of the stimulatory guanine-nucleotide-binding protein (Gs). *Biochem J*. 1989;262(2):643–649.
36. Lin F, et al. Gravin-mediated formation of signaling complexes in beta 2-adrenergic receptor desensitization and resensitization. *J Biol Chem*. 2000;275(25):19025–19034.
37. Nauert JB, et al. Gravin, an autoantigen recognized by serum from myasthenia gravis patients, is a kinase scaffold protein. *Curr Biol*. 1997;7(1):52–62.
38. Qasim H, McConnell BK. AKAP12 signaling complex: impacts of compartmentalizing cAMP-dependent signaling pathways in the heart and various signaling systems. *J Am Heart Assoc*. 2020;9(13):e016615.
39. Inokuma K, et al. Indispensable role of mitochondrial UCP1 for antiobesity effect of beta3-adrenergic stimulation. *Am J Physiol Endocrinol Metab*. 2006;290(5):E1014-21.
40. Chen HF, et al. CPEB2-dependent translation of long 3'-UTR Ucp1 mRNA promotes thermogenesis in brown adipose tissue. *EMBO J*. 2018;37(20):e99071.
41. Dai N, et al. IGF2BP2/IMP2-deficient mice resist obesity through enhanced translation of Ucp1 mRNA and other mRNAs encoding mitochondrial proteins. *Cell Metab*. 2015;21(4):609–621.
42. Villarroya F, et al. Transcriptional regulation of the uncoupling protein-1 gene. *Biochimie*. 2017;134:86–92.
43. Cao W, et al. p38 mitogen-activated protein kinase is the central regulator of cyclic AMP-dependent transcription of the brown fat uncoupling protein 1 gene. *Mol Cell Biol*. 2004;24(7):3057–3067.
44. Shen Y, et al. CRISPR-delivery particles targeting nuclear receptor-interacting protein 1 (*Nrip1*) in adipose cells to enhance energy expenditure. *J Biol Chem*. 2018;293(44):17291–17305.
45. Shamsi F, et al. FGF6 and FGF9 regulate UCP1 expression independent of brown adipogenesis. *Nat Commun*. 2020;11(1):1421.
46. Iida S, et al. PRDM16 enhances nuclear receptor-dependent transcription of the brown fat-specific Ucp1 gene through interactions with Mediator subunit MED1. *Genes Dev*. 2015;29(3):308–321.
47. He X, et al. Medicinal chemistry updates of novel

HDACs inhibitors (2020 to present). *Eur J Med Chem*. 2022;227:113946.
48. Martin MW, et al. Discovery of novel N-hydroxy-2-arylisoindoline-4-carboxamides as potent and selective inhibitors of HDAC11. *Bioorg Med Chem Lett*. 2018;28(12):2143–2147.
49. Shen S, Kozikowski AP. Why hydroxamates may not be the best histone deacetylase inhibitors — what some may have forgotten or would rather forget? *ChemMedChem*. 2016;11(1):15–21.
50. Doench JG, et al. Optimized sgRNA design to maximize activity and minimize off-target effects of CRISPR-Cas9. *Nat Biotechnol*. 2016;34(2):184–191.
51. Haeussler M, et al. Evaluation of off-target and on-target scoring algorithms and integration into the guide RNA selection tool CRISPOR. *Genome Biol*. 2016;17(1):148.